Accurate DC Current Ratio Measurements for Primary Currents up to 600 A

Gert Rietveld, *Senior Member, IEEE*, Jan H. N. van der Beek, and Ernest Houtzager, *Senior Member, IEEE*

***Abstract*— A setup based on a direct current (dc) comparator, typically employed in high-current low-resistance calibrations, has been developed for the accurate calibration of dc current ratios for dc currents up to 600 A. For primary currents above 100 A, multiple turns of the primary conductor are made through the device under test. A full uncertainty analysis reveals that the 1 part in 10^6 total expanded uncertainty ($k = 2$) in a calibration of a zero-flux device is limited by the behavior of the device, in particular the instability and sensitivity to the position of the primary current conductor.**

***Index Terms*— Current comparator, current measurements, current scaling, current transformers, dc current, measurement uncertainty, metrology, precision measurement.**

I. Introduction

ACCURATE measurements of large direct current (dc) are important for heavy industry, where high dc currents are, for example, used in production of aluminum and other electrochemical processes. Another important application is metering in dc electricity grids. High voltage dc links are increasingly being used to transport large amounts of energy over long distances and for connecting islands and offshore wind parks to the main electricity grid via underwater cables [1]. Furthermore, dc currents are used in science, especially for the generation of very strong magnetic fields, such as used at Conseil Européen pour la Recherche Nucléaire. Control of these fields requires dc current measurements at the best uncertainty levels [2]–[4].

A frequently used method for the accurate measurement of dc currents relies on shunts: low-ohmic resistors with down to $\mu\Omega$ values that convert the dc current into a dc voltage. The problem with this approach is heating of the shunt due to power dissipation of the high current that is to be measured. When using this approach in practice, a balance needs to be found between a significant signal voltage and limited power dissipation [5]. Especially for very large dc currents this becomes a problem since the output voltage scales linearly with current whereas the dissipation increases with the square of the current.

A second method for the accurate measurement of large dc currents scales this current down to lower values using a dc current transformer (DCCT) [6], [7]. This smaller current then again can be converted to a voltage, however, now a higher ohmic resistor can be used with less dissipation in the resistor. Presently, several commercial devices are available based on the DCCT technique [8].[1] This technique allows for reaching relative accuracies in the parts per 10^6 range, with even better nonlinearities. For calibration of such devices, reference setups with uncertainties of 1 part in 10^6 or better are required.

This paper describes a new facility for accurate calibration of commercial DCCTs and other dc current ratio devices designed for the measurement of large dc currents. First, the general measurement approach is described, which is a variant of a technique used in low resistance measurements at high currents, followed by details of the implementation of the method. Subsequently, measurement results are presented on the calibration of a commercial dc current ratio device using the new setup as well as the uncertainty in this measurement. In the conclusion, we summarize the results and indicate how the setup can also be used for absolute dc current measurements.

II. Measurement Approach

The best uncertainties in current ratio calibrations are achieved with cryogenic current comparators (CCCs) [9]. Their accuracy relies on the use of the perfect diamagnetism of superconductors, the so-called Meissner effect, together with superconducting quantum interference devices (SQUIDs) as sensor of the magnetic flux generated by the ampere-turn unbalance of the currents to be compared with each other. Whereas CCCs are typically designed for operation at currents of 1 A and below, an application up to 100 A has also been reported [10]. However, since CCCs require cryogenic liquids for their operation they are not very convenient for regular calibration of dc current ratio devices. In addition, the calibration of large dc currents does not require the ultimate magnetic flux sensitivity that SQUIDs provide.

As an alternative to CCCs, room-temperature current comparators (RTCCs) can be used that exploit a ferromagnetic core with flux modulation techniques [11]. RTCCs can achieve uncertainties in the parts per 10^8 range, which is by far sufficient for covering industrial needs. Even though RTCCs still are complex instruments, they can be readily automated and thus are very suitable for performing regular calibrations. The main applications of RTCCs are

Manuscript received February 4, 2015; revised March 21, 2015; accepted April 1, 2015. Date of publication June 2, 2015; date of current version October 7, 2015. This work was supported by the Dutch Ministry of Economic Affairs. The Associate Editor coordinating the review process was Dr. Branislav Djokic. *(Corresponding author: Gert Rietveld.)*

The authors are with the Van Swinden Laboratorium, Delft 2600AR, The Netherlands (e-mail: grietveld@vsl.nl).

Color versions of one or more of the figures in this paper are available online at http://ieeexplore.ieee.org.

Digital Object Identifier 10.1109/TIM.2015.2434096

[1]The manufacturers and instrumentation mentioned in this paper do not indicate any preference by the authors, nor do they indicate that these are the best available for the application discussed.

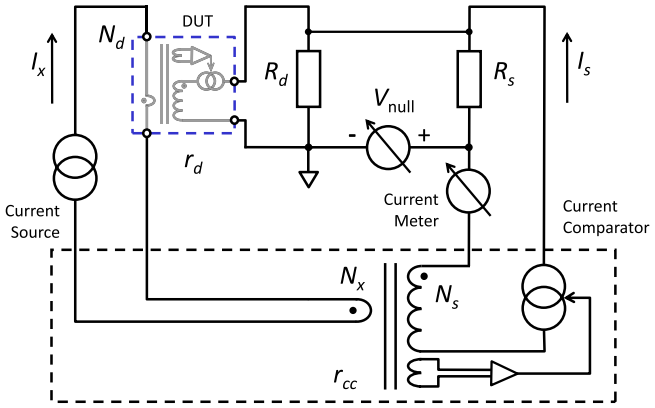

Fig. 1. Schematic of the high-current dc current ratio measurement bridge based on a RTCC (bottom dashed box). This dc current comparator balances the dc currents I_x and I_s in the two arms of the bridge. The top dashed box indicates the DUT, a dc current ratio instrument (e.g., based on a dc current comparator technique). The resistors R_d and R_s are used to convert the secondary currents to a measurement voltage. The bridge unbalance is detected with a nanovoltmeter.

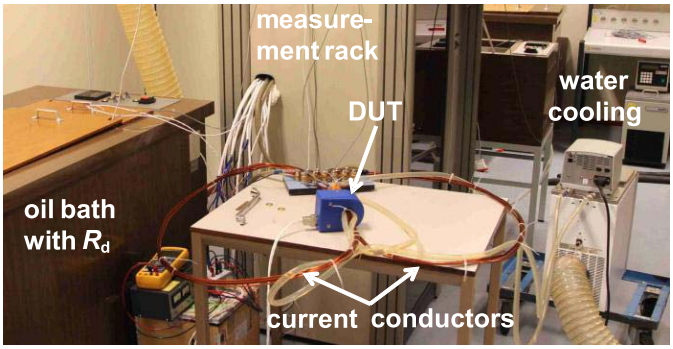

Fig. 2. Photograph of the setup, showing the oil bath containing R_d (left), the DUT and the primary conductors, the measurement rack (back), and the water cooling (right). The rack contains the high-current source I_x, voltage null detector, current meter, current comparator, and R_s.

in resistance measurements [12]–[14] and current ratio calibrations [6], [7], [15], [16]. The setup described in this paper applies a commercially available RTCC for the provision of traceability of large dc currents. It is based on a low-ohmic resistance bridge developed earlier [17], designed for the dc measurement of low-ohmic resistors and high current shunts.

A schematic of the adapted version of the setup suitable for the calibration of dc current ratio devices is given in Fig. 1. In the regular resistance bridge, a high current passes through the unknown resistor and compares the resulting voltage with the voltage across a reference resistor R_s in the other arm of the bridge. In the adapted dc current ratio calibration bridge, the high current passes through the unknown dc current ratio device and its low current output is converted to a voltage using an auxiliary resistor R_d. This voltage is again compared with that across the reference resistor R_s. A significant difference with respect to the resistance bridge is that both resistors R_d and R_s carry small currents and thus suffer less from dissipation effects.

The dc current ratio calibration bridge is effectively comparing the unknown current ratio r_d of the device under test (DUT) with the calibrated reference ratio r_{cc} of the dc current comparator in the measurement bridge. Using the ampere-turn balance

$$I_s \cdot N_s = I_x \cdot N_x \tag{1}$$

that is maintained by the internal feedback loop in this comparator (see Fig. 1), the unknown dc current ratio r_d of the DUT can be expressed as [18]

$$r_d = r_{cc} \cdot (R_s/R_d) + V_{null}/(R_d \cdot I_x) \tag{2}$$

with V_{null} the reading of the voltage null detector in the bridge.

When the unknown ratio r_d is nominally equal to r_{cc}, the values of R_s and R_d should be taken equal. More generally, the nominal ratio of R_s/R_d should equal the nominal ratio of r_d/r_{cc}. In this case, the voltage reading of the null detector V_{null} remains small, making the second term on the right hand side in (2) small. The measurement uncertainty then will mainly depend on the calibration of the resistors R_s and R_d, and of the ratio r_{cc} of the internal dc current comparator.

III. Implementation of the Method

A 19 rack contains the main elements of the setup: the current comparator with winding ratio r_{cc} and internal 100 mA current source, a high current source for generating I_x, a current meter for measurement of I_s, and a nanovoltmeter for measurement of the bridge unbalance. The measurement of I_s is needed to determine I_x in the second term on the right hand side in (2).

Special attention was paid to grounding and shielding in the setup. The low-current part of the setup is grounded at the low terminal of the nanovoltmeter (see Fig. 1). The exact grounding point of the primary current circuit is less critical and was placed at one of the output terminals of the I_x current source. All connections in the secondary low-current circuit of the setup are made with twisted-pair high-quality measurement cables. This minimized thermal voltages in the secondary circuit, and connecting the cable shields to the central ground point furthermore minimized electromagnetic interference and pickup of unwanted signals.

DC current ratio devices typically use a modulation technique for scaling the primary current to a lower value. To prevent that unavoidable residual modulation currents in the device output current affect the measurement uncertainty, a nanovoltmeter with a high normal mode rejection ratio (NMRR) and sufficient integration time has to be used. The Agilent 34420 nanovoltmeter used in our bridge has a specified NMRR of at least 80 dB, and was set to an integration time of 20 power line cycles (400 ms), so that even if residual modulation currents amount up to a few parts in 10^5 of the main current, this will not significantly affect the measurement uncertainty.

The measurement rack is located in a temperature-controlled shielded room that also contains the reference resistor R_s and

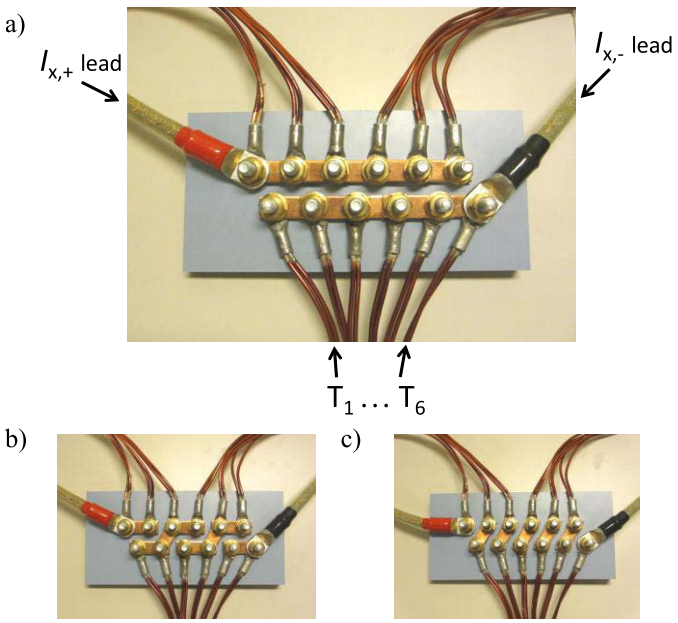

Fig. 3. (a) Parallel configuration of the six conductors $T_1, \ldots, T_6$ through the DUT to create an effective single turn (detail of Fig. 2). (b) and (c) Configuration for creating 3 turns and 6 turns, respectively.

an oil bath with the resistor R_d (see Fig. 2). Special attention is paid to the configuration and temperature control of the high-current carrying conductors. Further details of the setup are given in the following sections.

A. Measurement for Currents Above 100 A

The present high dc current source in the setup is a low-noise linear supply (Hewlett Packard model 6672A) that can generate I_x currents up to 100 A at a maximum compliance voltage of 20 V. To calibrate DUTs at higher currents, multiple turns of the primary I_x current lead are made through the center hole of the DUT [19]. With N_d primary turns through the DUT, the effective current seen by the device is $N_d \cdot I_x$ ampere-turns (A·t). In practice, the limit in effective current that can be realized with this method will be set by among others the amount of turns N_d that physically fit through the center hole of the DUT, and the maximum compliance voltage of the high-current source. By selecting the proper diameter of the primary current conductors, it should be possible to find an optimum where both effects together form a limiting factor. So far, the maximum current tested in our setup is equivalent to 600 A·t (6 turns at 100 A). With the 1.2-mΩ current conductors depicted in Fig. 3, neither the DUT inner hole dimensions nor the compliance voltage of the current source was a limiting factor.

To easily realize different numbers of primary turns, six conductors are placed though the DUT with the beginning and end of each conductor located close to each other. The conductors have a fixed mechanical position throughout the calibration with respect to the DUT, both in the DUT central hole as well as the distance of the return current conductors from the DUT. With copper strips the conductors can be either configured all in parallel (single turn), in series–parallel (two or three turns), or in series (six turns). Fig. 3(a) shows how the single-turn configuration is realized. Here, all + connections of each conductor are connected to the + connection of the current source, and similarly for the − connections.

Fig. 3(b) and (c) shows the configurations of the copper strips for the realization of 3 and 6 turns, respectively. In all cases, the current through each individual conductor is equal, except for small differences caused by contact resistances. Since each side of the DUT has three return conductors (see Fig. 2), the arrangement of the return current always is essentially symmetric with respect to the DUT.

B. Selection of Measurement Resistors

The selection of the resistor values of R_s and R_d depends on the current ratios to be calibrated. For the typical large currents that are to be calibrated, 10 A and higher, the current comparator reference ratio r_{cc} is set to 1:1000. With the reference resistor R_s taken as 1 Ω, the dissipation in R_s is not exceeding 10 mW up to the maximum primary current I_x of 100 A. If the DUT also has a nominal ratio of 1:1000, R_d is taken as 1 Ω as well.

For DUTs with different dc current ratios, the value of R_d is adjusted such that the R_s/R_d ratio equals the ratio r_d/r_{cc}. For calibrations above 100 A, when multiple primary turns are used for the DUT, the value of R_d has to be reduced accordingly. So for a DUT with $r_d = 1 : 1500$ and $1, 3$, and 6 primary turns, respectively, the nominal value of R_d that is to be used becomes 1.50, 0.50, and 0.25 Ω, respectively. In practice, these resistance values are realized via parallel and series–parallel connection of several model 4020B Leeds & Northrup 1 Ω resistance standards placed in an oil bath with temperature stability of a few millikelvin over 1 week. Low-ohmic connections between the current terminals of these resistors are realized with solid copper strips, and attention is paid to achieve a well-defined four-terminal resistance value.

C. Stray Fields

Since dc current ratio devices rely on sensing the magnetic flux generated by the primary current applied to them, they can exhibit an unwanted sensitivity to external stray fields as well. The extent to which external fields affect the accuracy of the calibration of these devices strongly depends on among others their design and (shielding) construction, the quality of the magnetic materials used, and on the configuration of the primary current conductors during the calibration. The effect of the primary current conductor configuration first of all includes their positioning in the central hole of the DUT: special attention should be paid to centering the current conductors in the middle of this hole, since off-centric positioning may lead to local saturation of the magnetic sensing core. Furthermore, the primary return current should be sufficiently far away from the DUT and moreover be symmetric with respect to the DUT. As can be observed in Fig. 2, this is realized in our setup by having 3 return conductors on each side of the DUT at the same, relatively large, distance. In this way, the stray fields of the return currents at the location

of the DUT are small and furthermore they more or less cancel out.

D. Environment

All measurements are performed in a shielded room with the temperature controlled to (23.0 ± 0.2) °C and the humidity controlled to $(45 \pm 5)\%$. Additional water cooling is arranged for keeping the primary conductor at the position of the DUT at the temperature of the environment. The cooling water is flowing through flexible silicon tubes that are running through the center hole of the DUT between the current conductors and the DUT. To reach a more homogeneous temperature at the inner wall of the DUT center hole, copper foil is wrapped around the total of current conductors and cooling tubes.

During a calibration, the temperature is measured at several locations using a thermistor-based temperature monitoring system with an overall measurement uncertainty of 20 and 45 mK ($k = 2$) for measurements in oil and air, respectively. These locations include the environment, the copper foil containing the current conductors and cooling tubes in the center hole of the DUT (mentioned in the previous paragraph), and the resistors R_s and R_d. For each current and each primary turn configuration, the temperature of the cooling water is adjusted such that the temperature of the primary conductor at the location of the DUT is within 1 °C equal to 23 °C.

E. Measurement Sequence

A calibration of the DUT starts with making the primary conductor configuration, as shown in Fig. 2. Then, the dc calibration current is applied and the water cooling adjusted to have a primary conductor temperature of approximately 23 °C. The right nominal value of R_d is realized and subsequently R_d and R_s are calibrated separately against a 1 Ω reference standard using a separate current comparator bridge. In principle, some time could be gained by directly calibrating the ratio R_d/R_s, since it is this ratio that enters the determination of the unknown r_d according to (2), but then no information is obtained on the individual stability of R_d and R_s.

The actual calibration of the DUT is done using a slightly adapted version of the measurement software described in [17]. To minimize the effect of thermal voltages, current reversal (sequence $+I$, $-I$, $+I$) is used to determine r_d at a certain current I. The most significant change to the measurement software is that the value of r_d can also be separately determined for positive and negative currents (sequence $0, +I, 0$ and $0, -I, 0$, respectively, to still minimize the effect of thermal voltages). In this way, the differences in ratio errors for positive and negative currents can be determined.

At the end of the measurements, R_d and R_s are calibrated again to determine any drifts due to instabilities or temperature changes.

IV. Measurement Results

To evaluate the capabilities of the dc current ratio calibration setup, it was used to calibrate a commercial dc current ratio device. The specific device selected was a Liaisons Electroniques Mecaniques model IT-600 S with nominal primary current range of 0–600 A [8], [20]. It is calibrated at 90, 300, and 600 A, respectively. The device is based on the zero-flux principle and has a nominal current ratio of 1:1500. The recommended burden (R_d) is 1.0 Ω, however, it must not exceed 2.5 Ω, corresponding to a maximum output compliance voltage of 1 V at 600 A primary current. In the present calibration, the maximum value of R_d was 1.5 Ω (see Section III-A), and the resulting output compliance voltage was either 90 or 100 mV which is well below the specified 1 V maximum.

TABLE I
Measured Ratio Deviation of a Commercial DC Current Ratio Instrument as a Function of Position of the Primary Current Conductor Within the Central Hole of the Device

Conductor position	Ratio deviation [10^{-6} from nominal]
Top	1.0
Right	0.7
Bottom	-0.6
Left	-0.5
Average	0.2
Centre	0.4

The following sections describe the results of the calibration of the dc current ration device and the associated verification measurements.

A. External Fields

When aiming for calibration uncertainties in the parts per 10^6 range, it is important to verify the effect of stray fields on the DUT, as well as the effect of the precise geometry of the magnetic fields generated by the primary current. The exact size of this effect depends on the magnetic properties of the internal magnetic core of the DUT and other details of its mechanical and electrical designs, and may manifest itself in two different ways. First of all, the calibration results may depend on the position of the primary current through the central hole of the DUT. If the primary current conductor is not exactly located in the middle of the DUT central hole, the magnetic fields generated by the current conductor will vary over the diameter of the DUT sensing element. Material inhomogeneities and imperfections in the (magnetic) shielding of the DUT sensing element may subsequently result in a different effective current ratio. In a more extreme situation, the magnetic core of the DUT may even become locally magnetized. To minimize the occurrence of such an effect in the present calibration, the DUT was switched OFF and ON before each measurement, to execute its initial demagnetization procedure. A second effect of the sensitivity to primary current field geometry is that the calibration results may depend on the configuration and distance of the return current conductors with respect to the DUT.

To quantify these effects for the DUT in the present calibration configuration, at the end of the calibration, the sensitivity of the DUT to the positioning of the primary

current conductors within the 25.4-mm central hole of the DUT is verified. The results of a test at 90 A current with all six conductors in parallel (see Fig. 3) are presented in Table I. The bundle of six conductors has a total diameter of around 15 mm. As can be observed in Table I, a significant variation of around 1.5 parts in 10^6 is found over the four conductor positions around the perimeter of the central hole. However, the average of the four measurements agrees very well within 0.2 part in 10^6 with the ratio deviation measured in the middle of the DUT central hole. This indicates that the effect of primary current conductor position for this particular DUT is well below 1 part in 10^6 when the conductor is reasonably carefully located in the middle of the DUT hole.

As a further test of the sensitivity of the DUT to external stray fields, the distance of the return current conductors with respect to the DUT has been reduced by roughly a factor of two, from 55 to 30 cm, without changing the position of the primary current conductors through the central hole of the DUT. The measurement results for these two return current conductor configurations agreed within the 0.1 part in 10^6 noise in each of the two measurements.

From the results of these two tests, we conclude that the effect of external stray fields on the calibrated ratio for this particular DUT, in the primary current conductor configuration used in the calibration, is less than 3 parts in 10^7.

B. Multiple Primary Conductor Turns

As a second step in the calibration process, the scaling or step-up using multiple primary turns is verified. This is done by comparing the DUT readings obtained with different turns but at the same ampere-turn signal: 1 turn at 90 A versus 3 turns at 30 A and 3 turns at 100 A versus 6 turns at 50 A. The different number of turns is realized, as described in Section III-A, using the connection panel shown in Fig. 3. It is important to note that the position of the primary current conductors in the central hole of the DUT does not change when changing the number of turns this way, nor does the position of the return current conductors. Therefore, only the effect of the scaling is measured and no additional effects caused by changing current conductor position come into play.

Fig. 4 shows the results of these tests. In principle, no effect should be seen since the DUT cannot discriminate the magnetic flux generated by a single conductor from the same flux generated by multiple conductors. For the present DUT, a small effect is seen, however, possibly related to the effect of primary current conductor positioning described in the previous section. The size of the effect is (0.54 ± 0.54) parts in 10^6 and (0.23 ± 0.28) parts in 10^6 ($k = 2$) for the 1 turn versus 3 turns at 90 A·t test and for the 3 turns versus 6 turns at 150 A·t test, respectively. The top graph of Fig. 4 shows that the 1 turn versus 3 turn measurement has a somewhat worse repeatability over several days (significantly worse than the repeatability on a single day), leading to a larger uncertainty in the determination of the deviation of this scaling step.

C. Calibration Results

The results shown in Fig. 4 already demonstrate the low noise of the bridge and the good reproducibility in the current

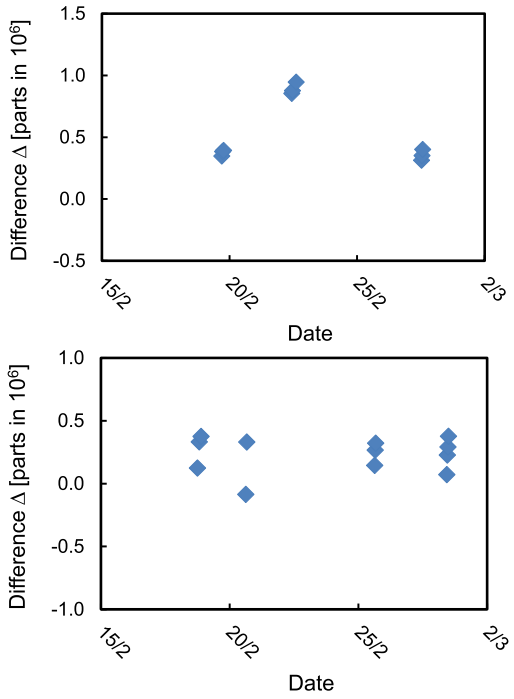

Fig. 4. Difference Δ between DUT calibration results achieved for different primary conductor turns but with the same ampere-turn signal: 1 turn at 90 A versus 3 turns at 30 A (top) and 3 turns at 100 A versus 6 turns at 50 A (bottom).

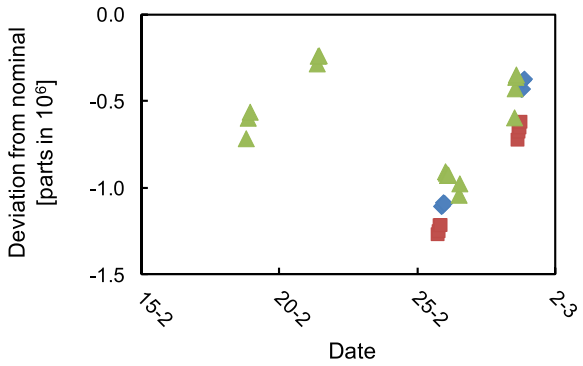

Fig. 5. Calibration results of the 1:1500 ratio of a dc current ratio transformer at 600 A·t (6 turns with 100 A current). Results are presented for reversed current (sequence $+I, -I, +I$; triangles), negative current (sequence $0, -I, 0$; squares), and positive current (sequence $0, +I, 0$; diamonds).

ratio measurements. Fig. 5 shows the calibration result of the DUT at 600 A·t using 6 primary conductor turns.

This result includes corrections for the effect of the multiple turns as well as corrections for temperature of R_d and R_s. The latter corrections arise from the different power consumptions during the calibration of the resistors and their subsequent use in the dc current ratio bridge. The temperature rise in R_d and R_s for this calibration was around 20 and 200 mK, respectively, which combined with the respective temperature coefficients of $+11$ and -1.5 $\mu\Omega/\Omega$/K results in a total correction of approximately -0.5 parts in 10^6. The measured deviation from nominal ratio at 600 A·t amounts to only -0.6 parts in 10^6 for reversed currents and essentially equal

TABLE II
UNCERTAINTY BUDGET FOR THE MEASURED RATIO DEVIATION OF A COMMERCIAL DC CURRENT RATIO INSTRUMENT AT 600 A·t BASED ON (3)

Quantity	Value	Standard Uncertainty	Distribution	Uncertainty Contribution
r_{cc}	$1.000000000 \cdot 10^{-3}$	$120 \cdot 10^{-12}$	normal	$80 \cdot 10^{-12}$
R_s	1.000003820 Ω	$124 \cdot 10^{-9}$ Ω	normal	$83 \cdot 10^{-12}$
R_d	0.249965350 Ω	$68.9 \cdot 10^{-9}$ Ω	normal	$180 \cdot 10^{-12}$
δ_{ratio}	$-142.300 \cdot 10^{-6}$	$250 \cdot 10^{-9}$	normal	$170 \cdot 10^{-12}$
δ_{ratioB}	0.0	$57.7 \cdot 10^{-9}$	rectangular	$38 \cdot 10^{-12}$
$\delta_{scaling}$	$-770 \cdot 10^{-9}$	$300 \cdot 10^{-9}$	normal	$200 \cdot 10^{-12}$
δ_{stray}	0.0	$173 \cdot 10^{-9}$	rectangular	$120 \cdot 10^{-12}$
r_{DUT}	$666.6662 \cdot 10^{-6}$			$360 \cdot 10^{-12}$

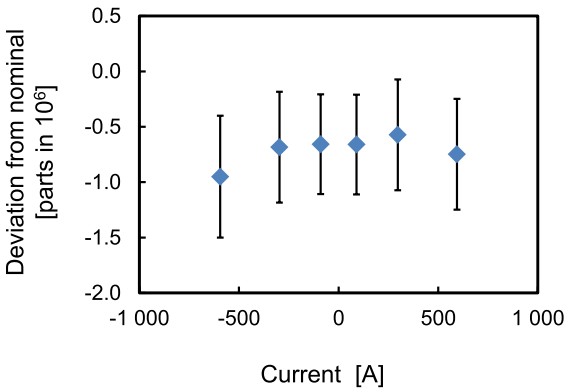

Fig. 6. Calibration results of the 1:1500 ratio of a dc current ratio instrument as function of applied equivalent current. Error bars indicate the combined standard uncertainty in the measurements ($k = 1$; see Table II for an example calculation).

(but slightly lower) values are found for positive and negative currents.

V. MEASUREMENT UNCERTAINTY

For estimation of the uncertainty in the dc current ratio calibrations, the following mathematical model is used:

$$r_{DUT} = r_{cc} \cdot (R_s / N_d \cdot R_d) \cdot (1 + \delta_{ratio} + \delta_{ratioB} + \delta_{scaling} + \delta_{stray}) \quad (3)$$

where δ_{ratio} is the measured bridge unbalance and δ_{ratioB} is the corresponding systematic uncertainty in this unbalance. The terms $\delta_{scaling}$ and δ_{stray} correspond to the uncertainties related to the current scaling using multiple primary conductor turns and the effect of stray fields, respectively, and have been determined in the experiments described in Section IV. The term δ_{ratio} includes the repeatability in the measurements (as shown in Fig. 5), whereas δ_{ratioB} is mainly determined by the 2 nV uncertainty in the gain calibration of the nanovoltmeter used as null detector. Since the null detector reading is always less than 100 mV, this 2 nV uncertainty contributes less than 1 part in 10^7 to the uncertainty budget.

The uncertainties of R_s and R_d include contributions from their calibration, stability, and temperature effects. The calibration is performed with a current-comparator resistance bridge resulting in 1 part in 10^7 uncertainty. The corrections for temperature effects on R_s and R_d are known with 5 part in 10^8 uncertainty. For R_d the most significant uncertainty comes from the stability: the value of R_d needs to be changed whenever the number of primary turns N_d is changed. It appears that in practice the instability of the contact resistance of the copper strips used to make the correct series/parallel configuration of the 1 Ω standards used for realizing R_d (as described in Section III-B) is the limiting factor in the determination of R_d. The low uncertainty in the determination of r_{cc} originates from a thorough verification in which the 1:10 and 1:100 ratio of this reference current comparator was compared with its 1:1000 ratio [21].

Table II gives the resulting uncertainty budget for the 600 A·t calibration shown in Fig. 5. The values of the standard uncertainties given in Table II are explained above; the uncertainty contributions are calculated by multiplying the standard uncertainties with their respective sensitivity factors using (3). The uncertainty budget clearly shows that the dominant contributions in the total 1.1 part in 10^6 expanded uncertainty ($k = 2$) originate from the DUT: instability, scaling, and position of the primary conductors. This is also the case for the calibrations at 90 and 300 A·t where slightly lower uncertainties are achieved. For a DUT with insignificant contribution to the uncertainty, and well stabilized R_d, a best expanded measurement uncertainty of 0.4 parts in 10^6 ($k = 2$) can be achieved.

The final result of the calibration is shown in Fig. 6. It can be seen that the results obtained at 90 and 300 A·t are within 0.3 parts in 10^6 equal to those at 600 A·t, well within the standard deviation of the measurements, showing that the DUT has an excellent linearity over 15% up to 100% of its full range.

VI. CONCLUSION

A setup has been developed for the accurate measurement of dc current ratio devices up to 600 A primary current. The setup is based on an existing low-ohmic resistance measurement bridge and can operate up to 100 A. One of its unique features is that it does not require the current ratio of the reference within the setup to be equal to that of the DUT. This makes the setup easy to use and flexible in its application.

At present, for calibration at currents above 100 A, multiple turns are applied through the DUT to increase the effective current seen by the DUT. In this way, using, for example, 6 turns, DUTs can be calibrated with an equivalent current of 600 A. Calibrations at even higher currents can be performed using a current source with higher maximum current output and/or using more primary turns. In practice, the maximum effective current that can be realized with the latter method will be set by the amount of primary turns that physically fit through the center hole of the DUT and the voltage compliance of the current source. Using current sources with higher output ranges may add to higher relative ripple in the current signal, which will lead to larger standard deviations

in the measurements and possibly also to systematic errors when the bandwidth of the DUT and the reference setup are different.

The capabilities of the new setup have been evaluated by calibrating a commercial dc current ratio device with nominal primary current range of 0–600 A at 90, 300, and 600 A, respectively. The deviation from nominal ratio at 600 A is only (-0.6 ± 1.1) part in 10^6 ($k = 2$), with similar values and uncertainties at 90 and 300 A. The uncertainties are dominated by imperfect behavior of the current ratio device; for better devices, uncertainties of 0.4 parts in 10^6 can be achieved. This is slightly better than the best uncertainties in dc current ratio calibrations claimed previously [22] and comparable with a recent claim [23].

REFERENCES

[1] R. Rudervall, J. P. Charpentier, and R. Sharma, "High voltage direct current (HVDC) transmission systems technology review paper," in *Proc. Energy Week*, Washington DC, USA, 2000, pp. 1–19.

[2] G. Fernqvist, B. Halvarsson, J. Pett, and J. Pickering, "A novel current calibration system up to 20 kA," *IEEE Trans. Instrum. Meas.*, vol. 52, no. 2, pp. 445–448, Apr. 2003.

[3] M. C. Bastos *et al.*, "High accuracy current measurement in the main power converters of the large hadron collider: Tutorial 53," *IEEE Instrum. Meas. Mag.*, vol. 17, no. 1, pp. 66–73, Feb. 2014.

[4] G. Hudson and K. Bouwknegt, "4–13 kA DC current transducers enabling accurate *in-situ* calibration for a new particle accelerator project, LHC," in *Proc. Eur. Conf. Power Electron. Appl. (EPE)*, 2005, pp. 1–8.

[5] M. Kraft, "Measurement techniques of low value high current single range current shunts from 15 amps to 3000 amps," *Measure*, Mar. 2007, vol. 2, no. 1, pp. 44–49.

[6] N. L. Kusters, "The precise measurement of current ratios," *IEEE Trans. Instrum. Meas.*, vol. IM-13, no. 4, pp. 197–209, Dec. 1964.

[7] M. P. MacMartin and N. L. Kusters, "A self-balancing direct current comparator for 20 000 amperes," *IEEE Trans. Magn.*, vol. 1, no. 4, pp. 396–402, Dec. 1965.

[8] [Online]. Available: http://www.lem.com, www.hitec-ups.com, www.guildline.com, and www.mintl.com, accessed Feb. 13, 2015.

[9] J. M. Williams, "Cryogenic current comparators and their application to electrical metrology," *IET Sci. Meas. Technol.*, vol. 5, no. 6, pp. 211–224, Nov. 2011.

[10] J. M. Williams and P. Kleinschmidt, "A cryogenic current comparator bridge for resistance measurements at currents of up to 100 A," *IEEE Trans. Instrum. Meas.*, vol. 48, no. 2, pp. 375–378, Apr. 1999.

[11] W. J. M. Moore and P. N. Miljanic, *The Current Comparator* (IEE Electrical Measurement Series), vol. 4. London, U.K.: Peregrinus, 1988.

[12] M. P. MacMartin and N. L. Kusters, "A direct-current-comparator ratio bridge for four-terminal resistance measurements," *IEEE Trans. Instrum. Meas.*, vol. 15, no. 4, pp. 212–220, Dec. 1966.

[13] N. L. Kusters and M. P. MacMartin, "A direct-current-comparator bridge for measuring shunts up to 20000 amperes," *IEEE Trans. Instrum. Meas.*, vol. 18, no. 4, pp. 266–271, Dec. 1969.

[14] K.-T. Kim, J. K. Jung, Y. Lee, and E. So, "The establishment of high current DC shunt calibration system at KRISS and comparison with NRC," in *Proc. Conf. Precis. Electromagn. Meas. (CPEM)*, Aug. 2014, pp. 614–615.

[15] G. Fernqvist, H.-E. Jorgensen, and A. Saab, "Design and verification of a 24 kA calibration head for a DCCT test facility [LHC current control]," *IEEE Trans. Instrum. Meas.*, vol. 48, no. 2, pp. 346–350, Apr. 1999.

[16] H. Shao *et al.*, "DC 5 kA current ratio standards based on series–parallel self-calibration DCCs," *IEEE Trans. Instrum. Meas.*, vol. 62, no. 11, pp. 3093–3100, Nov. 2013.

[17] E. Houtzager and G. Rietveld, "Automated low-ohmic resistance measurements at the $\mu\Omega/\Omega$ level," *IEEE Trans. Instrum. Meas.*, vol. 56, no. 2, pp. 406–409, Apr. 2007.

[18] G. Rietveld, J. van der Beek, and E. Houtzager, "Accurate high-current DC current ratio measurements," in *Proc. Conf. Precis. Electromagn. Meas. (CPEM)*, Aug. 2014, pp. 610–611.

[19] B. Jeckelmann, "Genauigkeit von Gleichstrom-messungen bis 20 kA im ppm-Bereich," *metINFO Zeitschrift Metrol.*, vol. 11, no. 3, pp. 4–8, 2004.

[20] W. Teppan and D. Azzoni, "Closed-loop fluxgate current sensor," European Patent WO 2010/131 187, Nov. 18, 2010.

[21] G. Rietveld, J. H. N. van der Beek, M. Kraft, R. E. Elmquist, A. Mortara, and B. Jeckelmann, "Low-ohmic resistance comparison: Measurement capabilities and resistor traveling behavior," *IEEE Trans. Instrum. Meas.*, vol. 62, no. 6, pp. 1723–1728, Jun. 2013.

[22] G. Hudson, B. Jeckelmann, and J.-D. Baumgartner, "Comparison of CERN and metas high current standards up to 10 kA," in *CPEM Conf. Dig.*, Jun. 2008, pp. 548–549.

[23] L. Callegaro, C. Cassiago, and E. Gasparotto, "On the calibration of direct-current current transformers (DCCT)," *IEEE Trans. Instrum. Meas.*, vol. 64, no. 3, pp. 723–727, Mar. 2015.

Gert Rietveld (M'10–SM'12) was born in The Netherlands in 1965. He received the M.Sc. (*cum laude*) and Ph.D. degrees in low temperature and solid-state physics from the Delft University of Technology, Delft, The Netherlands, in 1988 and 1993, respectively.

He joined the Van Swinden Laboratorium (VSL), Delft, in 1993, where he is currently a Senior Scientist with the DC/LF Group, Department of Research and Development. As a Program Manager, he has coordinated the scientific work of all technological areas within VSL. He recently coordinated a 22-partner European joint research project on smart grid metrology. His current research interests include the development of power measurement systems, smart grid metrology, and electrical quantum standards, in particular, the quantum Hall resistance standard.

Dr. Rietveld is a member of the International Committee for Weights and Measures and the Chair of its Consultative Committee for Electricity and Magnetism (CCEM). Furthermore, he is the VSL Contact Person on the Technical Committee of Electricity and Magnetism of the European Association of National Metrology Institutes (EURAMET), the Founding Chair of the EURAMET Expert Group on Power and Energy, and a Secretary and member of several CCEM, EURAMET, CIGRÉ, and the IEEE working groups.

Jan H. N. van der Beek was born in Rijswijk, The Netherlands, in 1960. He received the (*cum laude*) B.Sc. degree in electronics from MTS-Leyweg, Hague, The Netherlands, in 1989.

He joined the Van Swinden Laboratorium, Delft, The Netherlands, in 1989, after his studies, where he specialized in impedance measurements, multifunction and dc voltage measurements, and high ohmic dc resistance. His current research interests include dc voltage and dc resistance.

Ernest Houtzager (M'11–SM'12) was born in Hilversum, The Netherlands, in 1978. He received the B.Sc. degree in electronics from Hanze University Groningen, Groningen, The Netherlands, in 2001.

He joined the Van Swinden Laboratorium, Delft, The Netherlands, in 2001, after his studies, where he specialized in high-frequency measurements and direct-current resistance measurements, including quantum Hall resistance, and furthermore involved in the development of a quantum alternating-current voltage standard (i.e., the Josephson arbitrary waveform synthesizer). His current research interests include high voltage and low frequency power measurements.